Interdisciplinary Journal of Applied and Basic Subjects (2021), 1(11), 16-26
ISSN 2583-052X

RESEARCH PAPER

Article Identifier: https://identifier.visnav.in/1.0002/ijabs-21j-27015/

Aeromagnetic data investigations of the potential mineralized zones in parts of Zuru schist belt, Northwestern Nigeria

Abubakar Isah [1*], Kazeem Salako[2], Mustapha Abbas [1], A. Saleh [3] and A. Dahiru [1]

[1] Department of Physics, Faculty of Physical Sciences, Kebbi State University of Science and Technology, Aliero, Kebbi State, Nigeria
[2] Department of Physics, Federal University of Technology Minna
[3] Physics Unit, School Preliminary and Continuing Education, Ibrahim Badamasi Babangida University Lapai

For correspondence: abubakariash682@gmail.com

ABSTRACT

The study area is located within the north-western Nigeria, Zuru schists belt, bounded by latitudes 11°-12° N and longitudes 5°-6° E with a total surface area of 21,000 km^2. The qualitative interpretation of the total field anomaly was carried-out using analytic signal, reduced to pole and first vertical derivative techniques. These techniques enhanced the visualization of the structural features such as faults and folds which are capable of hosting mineralized deposits within the studied region. More so, quantitative interpretation of the total field anomaly reveals the depth extents to the potential mineralized zones, with values in the range of 134.2 to 339.6 m, which were computed from the 3-D Euler deconvolution technique. The overall results of the qualitative and quantitative analyses are synonymous and thus reveal that the study area is affected by the NNE-SSW, NE-SW, N-S and E-W trends. Hence, the potential mineralized zones within the study area are structurally controlled along the Eburnean deformation (D1) and Pan-African (D2) deformation episodes.

Keywords: Aeromagnetic, north-western Nigeria, Eburnean deformation, Zuru schists

1. INTRODUCTION

The search for mineral resources that are concealed within the subsurface of the earth is of great importance to geoscientist. The existences and extent of these mineral resources can only be established via the application of geophysical probes of the structural features within an area. Aeromagnetic is one of the cost-effective and rapid geophysical survey methods that aids in probing the subsurface of the earth for mineral resources exploration [1]. There are various aeromagnetic data interpretation

techniques such as total gradient amplitude, horizontal gradient amplitude, vertical derivatives, tilt derivatives among others that have been used to map the lateral boundaries of the magnetic anomalies [2-4]. On the other hand, the depth extent to the magnetic source has been estimated using numerous methods such as 3-D Euler deconvolution, source parameter imaging, spectral analysis [5]. Several geophysical studies in parts of the study area have been carried-out for example; Salawu *et al*. (2019) detected the edge and also estimate the magnetic basement depth of Danko situated within northwestern Nigeria using aeromagnetic data [5]. Umaru (2016) incorporated the geochemical analysis, aeromagnetic, topographic dataset to interpret the geology and structural evolution of Danko in the south-western part of Zuru schist belt, northwestern Nigeria [6]. Binta *et al.* (2016) reported the economic beneficiation of low-grade manganese ore from Wasagu area, northwestern Nigeria [7].

The present study area falls within the Zuru schist belt. The Zuru schist belt host the regional the transcurrent Anka-Yauri shear system of the northwestern crystalline basement complex [8]. This shear system is believed to be a host of numerous mineral deposits such gold, manganese, copper among others within numerous structural features (such as faults, fractures, folds and shear zones) [8]. These structural geologic features perhaps serve as conduits for the transportation and accumulation of mineral deposits [9]. The study region has not been well captured for geophysical studies and has over a decade act as host for artisanal mining activities. These artisanal mining activities lack the exact structural configuration of their primary targets. Thus, mostly adopted the trial-and-error excavations. Thereby, leading to the destruction of natural flora and fauna, landscape degradations, flooding, erosion as well as

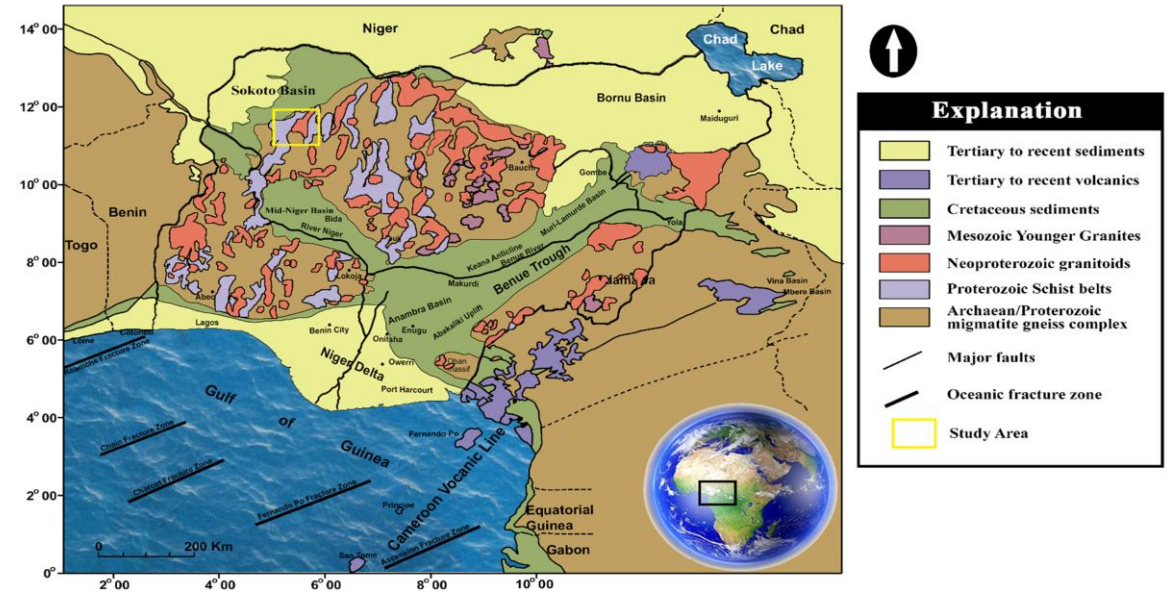

Figure 1. The Nigeria geological map and its environs showing the study area indicated with black square box.

release of toxic waste into air and waterways.

In this regard, the present study employed analytical signal, reduce to pole, first vertical derivative (FVD) and 3-D Euler deconvolution techniques to delineate and estimate the depths extent to the top of subtle geological sources beneath the study area. Therefore, the study tends to investigate the potential mineralized zones in parts of Zuru schist belts, north-western Nigeria.

1.1. Geology of the Study Area

The studied region is bounded between Latitudes 11° to 12° N and Longitudes 5° to 6° E (Fig. 1) with an estimated surface area of 12,100 Km^2, within the Proterozoic Zuru schist belt. The belt comprises of muscovite schists and quartzites, with minor quartz and pegmatite veins [10] (Fig. 1). The Zuru belt is perhaps the largest schist belt in north-western Nigeria, with a length of about 280 Km and a width of about 40 km [11]. Structurally, the Zuru schist belt is located in a strained region, where rock units are affected by two deformation events [12]. Although, the deformation configuration exposed within the region is relatively complicated with changeable geologic features [13]. The N-trending geologic structures (Pan-African) are overlaid on beddings in relation to the older Palaeo to Mid- Proterozoic (Eburnean) folds with the E trends

2. METHOD AND MATERIALS

2.1. Data Source

The study area was covered by four data sheets of the total field intensity. These are numbers 74, 75, 97 and 98 on a scale of 1: 100,000. The aeromagnetic data was obtained from the Nigeria geological survey Agency (NGSA), as part of the nation-wide aeromagnetic survey between 2004 and 2009. The aeromagnetic data were collected at a nominal flight altitude of 80 m along approximately N-S flight (nearly perpendicular to predicted geological strikes in the area), a spacing of 2 km was used. Diurnal and international Geomagnetic Reference Field (IGRF) where correction was both carried out on the aeromagnetic data.

2.2. Data collection

The processing of the total field anomaly data of the study area includes; (a) the TFA data was subjected to the 3-D Euler deconvolution technique to produce the clusters of depth solutions. (b) the total field anomaly data were applied to analytic signal filter. Afterwards, automatic lineament extractions were carried out on the AS data using centre for exploration targeting (CET) of Geosoft software. Additionally, Rosette diagram was formed to understand the trend of the magnetic lineament using Rockworks software. (c) the total field anomaly data was reduced to pole prior to the first vertical derivative filter computations. (d) the depth extent to the concealed subsurface geologic features were estimated using the 3-D Euler deconvolution method. The theories of the adopted methods are discussed below

2.3. *Detection of structural features*

The application of integrated filtering techniques in the delineation of the geologic features increases the mineral exploitation

opportunities than using a lone method. It is for this reason, the study employed several enhancement filters including; analytic signal, tilt derivative, first vertical derivative, centre for exploration targeting and thus, the depth extent to the mineralised deposits is estimated using 3D Euler deconvolution and source parameter imaging.

2.4. Analytic signal (AS)

This technique centres the peaks of the magnetic source anomalies over their respective causative sources at low latitude regions. The method is unlike to magnetic equator or reduces to the magnetic pole i.e. it does not require the direction of magnetisation source prior to the application of the filter [14]. The analytic signal filter is defined as the square root of the sum of the vertical and horizontal derivatives of magnetic field given as thus [15]:

$$AS(x,y) = \sqrt{\left(\frac{\partial F}{\partial x}\right)^2 + \left(\frac{\partial F}{\partial y}\right)^2 + \left(\frac{\partial F}{\partial z}\right)^2} \quad ..eq.\ 1$$

Where:

AS = total field anomaly data (given as;AS (x, y))

F= airborne magnetic anomaly field (observed at (x, y)).

2.5. *First* vertical derivative (FVD)

The first vertical derivative (FVD) is a high pass filter applied to the RTP data to calculate its gradient vertically. The FVD refines the effect of high frequency (short wavelength) magnetic features. It is also useful for enhancing the textural variation in the data.

$$L(r)=r^n \quad ...eq.\ 2$$

Where:

n = order of differentiation.

2.6. 3-D Euler *Deconvolution (ED)*

3-D Euler deconvolution (ED) method requires the total field anomaly data to estimate the depths and locations of the magnetic source anomalies, since it does not depend on the direction of magnetisation. The 3-D Euler deconvolution is based on the Euler's homogeneity equation [15] given as thus:

$$(x-x_0)\frac{\partial F}{\partial x} + (y-y_0)\frac{\partial F}{\partial y} + (z-z_0)\frac{\partial F}{\partial z} = N(B-F) \quad ...eq\ 3$$

where, x_0, y_0 and z_0 are the position or coordinate of the top magnetic source, (x, y, z) are the location of the field measurement, T is the total field anomaly value, B is the background field, ∂T/(∂x), ∂T/∂y and ∂T/∂z are the derivative of the total field values T and N is the degree of homogeneity is also referred to as structural index (SI) which is a measure of the rate of change with distance of a field [16].

3. RESULT AND DISCUSSION

3.1. *Qualitative interpretation of the structural geologic features*

3.1.1. Total field anomaly map

The total field anomaly map (Fig. 2) denotes the IGRF removed 33,000 nT of the study region, with magnetic anomalies values in the range of -14.5 to 88 nT. The TFA anomaly map represented in different colour aggregates accounts for the variations in amplitudes, wavelengths, depths, strike directions in rock

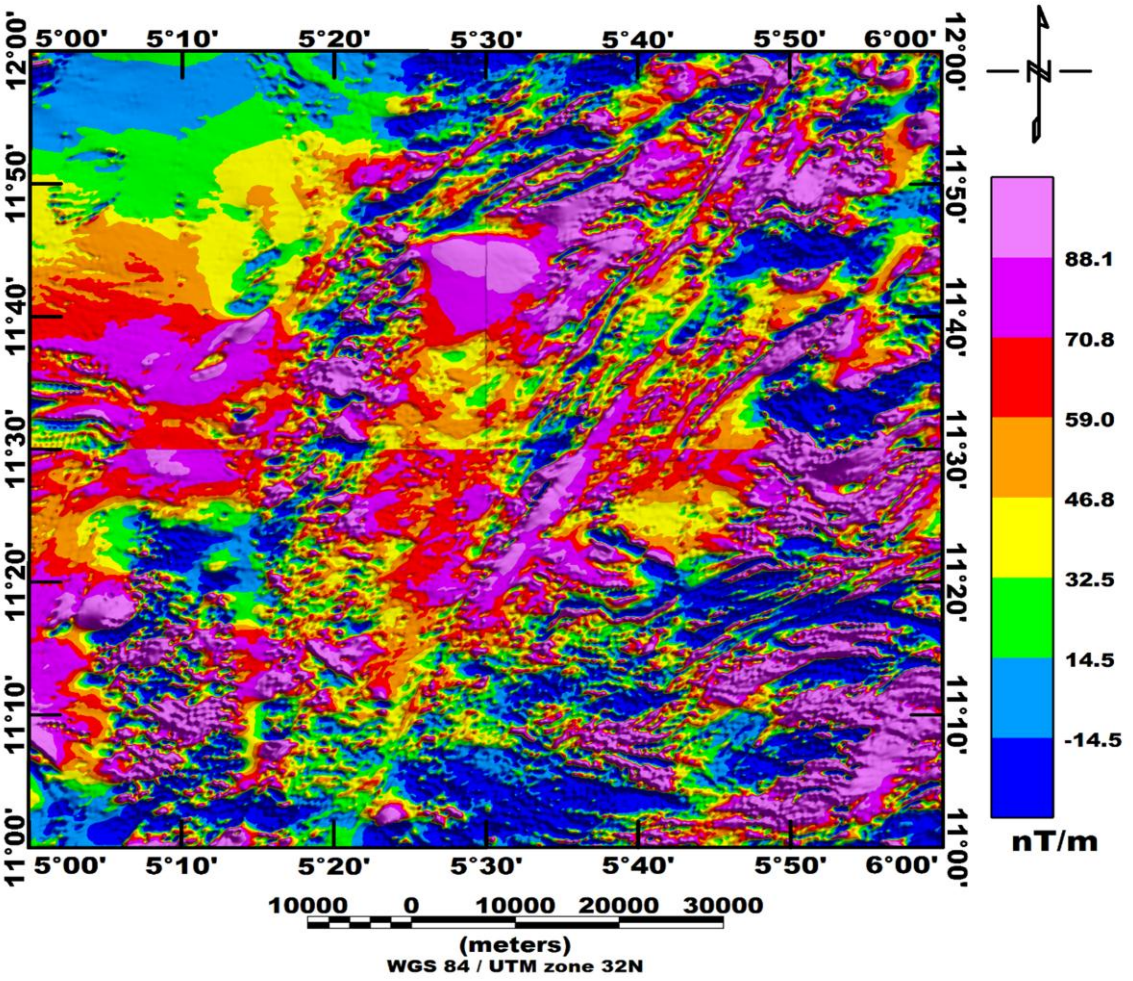

Figure 2. Total field anomaly map of the study area

units within the study region (Fig. 2). The TFA anomaly map pinpoints the fault-like structural geologic features which are broadly distributed throughout the entire study region. However, high amplitude magnetic anomaly in pink colour are prominently observed in the west southwest, central, east southeast and north north-eastern parts of the map. These high magnetic anomalies mainly have spherical, NE-SW and E-W trends. Meanwhile, low amplitude magnetic anomaly in blue colour is predominantly located toward the south southwest, south southeast and north north-western parts of the studied region with similar NE-SW and E-W trends. Since, the study area falls within the low latitude region, magnetic anomalies at this region inclined. Thus, the magnetic anomalies ought to be righteously place above their causative sources. This necessitates the use of reduce to pole and/or analytic signal filters.

3.1.2. Analytic signal map

The analytic signal is like reduce to pole filter which is applied at both high and low latitude region [14]. The analytic signal has an edge over

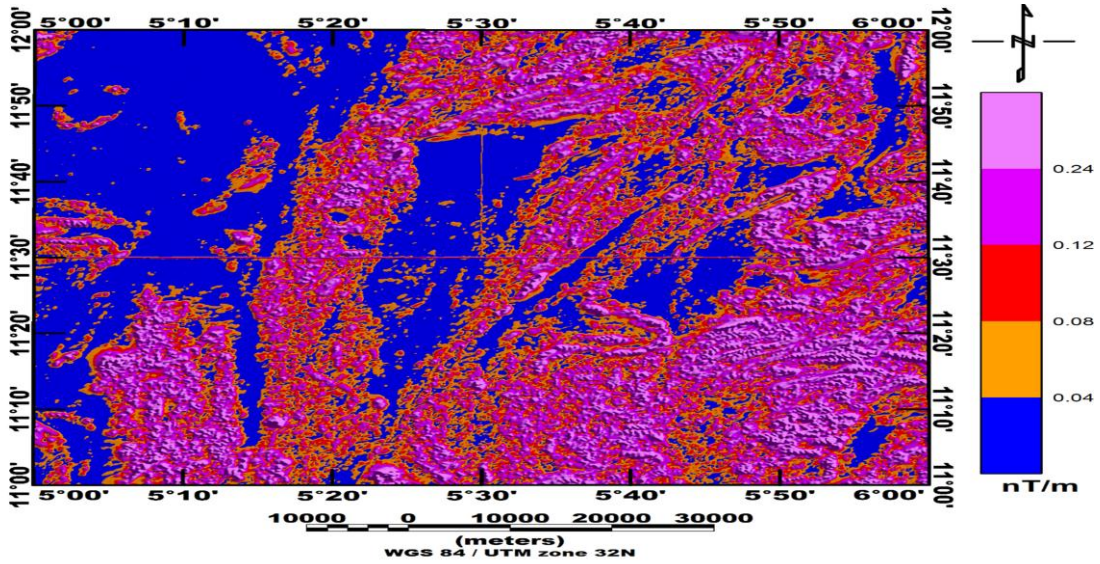

Figure 3a. Analytic signal anomaly map of the study area

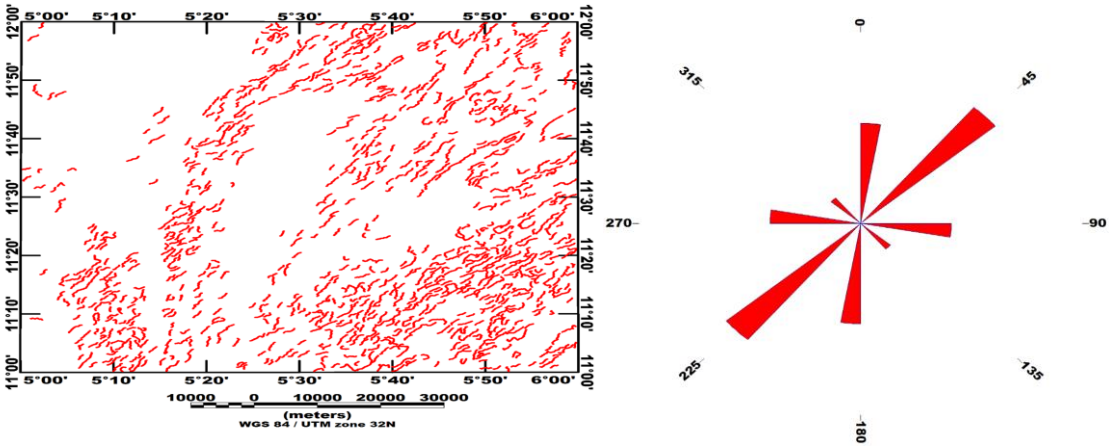

Figure 3b. (Left) Analytic signal structural lineaments map of the study area
Figure 3c. (Right) Rose diagram derived from analytic signal structural lineaments of the study area

reduce to pole or equator because it is independent on the direction of magnetisation for 2-D structural features [17].

Conversely, the analytic signal is dependent on the directions of source magnetisation and ambient magnetic field for the 3-D magnetic sources [17-18]. The visual inspection of the analytic signal map (Figure 3a) reveals both high and low magnetic anomalies which varies in the range of 0.04 to 0.24 nT/m. The regions of low analytic signal amplitudes in blue colour, particularly at the central and north north-western segments of the study region coincides with the relatively high total field anomaly map (Figure 2) and vice versa. Thus, implying that the magnetisations are possible weakened resulting to the meta sedimentary formations.

The high analytic signal amplitudes values were virtually observed all over the study area with the exception of the central north north-western and some central portions of the study area. This suggested that the locations of the high

analytic signal amplitudes have significant magnetic susceptibility differences and thus produced detectable magnetic structures over the study area. In an effort to depict the distributions of edges and horizontal extent, structural lineaments were extracted from the analytic signal anomaly map (Figure 3b). Hence, the Rose diagram (Figure 3c) of the analytic signal lineaments reveals that the dominant trends are in the NNE-SSW, NE-SW, N-S and E-W directions.

The reduced to pole map (Figure 4a) shows magnetic anomalies with both high and low configurations within the study area. The reduced to pole magnetic anomaly have values that vary in the range of – 85.6 to 10.5 nT. The high magnetic anomalies are represented in pink colour, which are more evident around the northern, southern and eastern segments of the study area. In contrast, areas of high magnetic

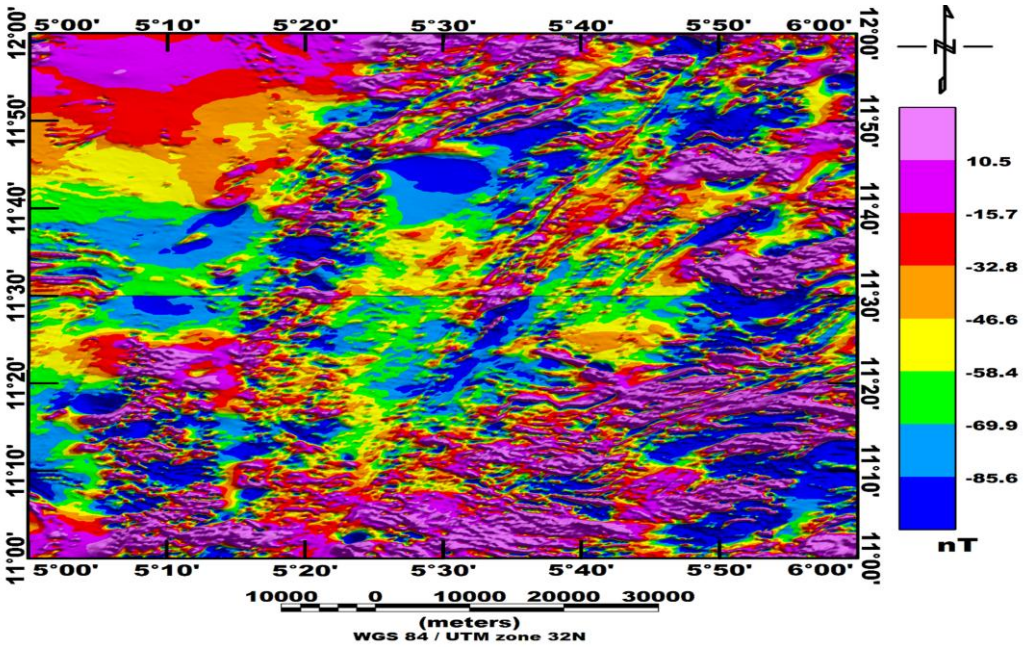

Figure 4a. Reduced to pole anomaly map of the study area

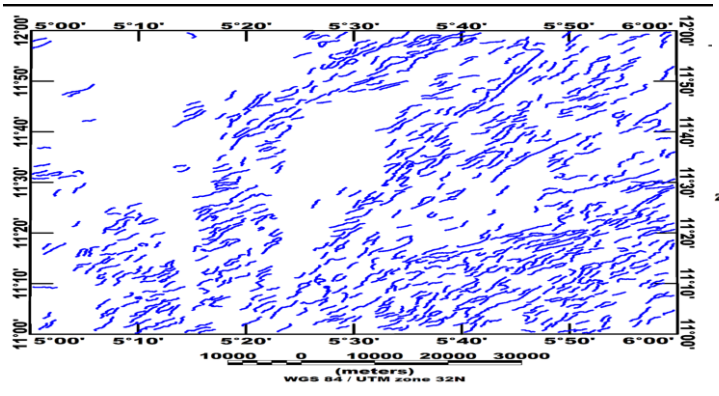

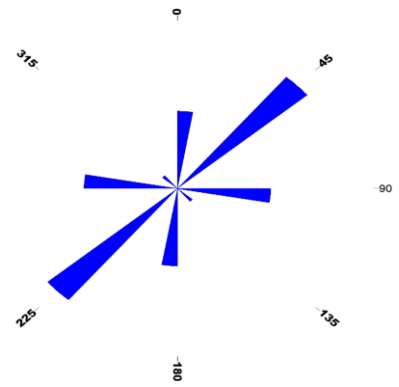

Figure 4b. (Left) Reduced to pole structural lineaments map of the study area
Figure 4c. (Right) Rose diagram derived from reduced to pole structural lineaments of the study area

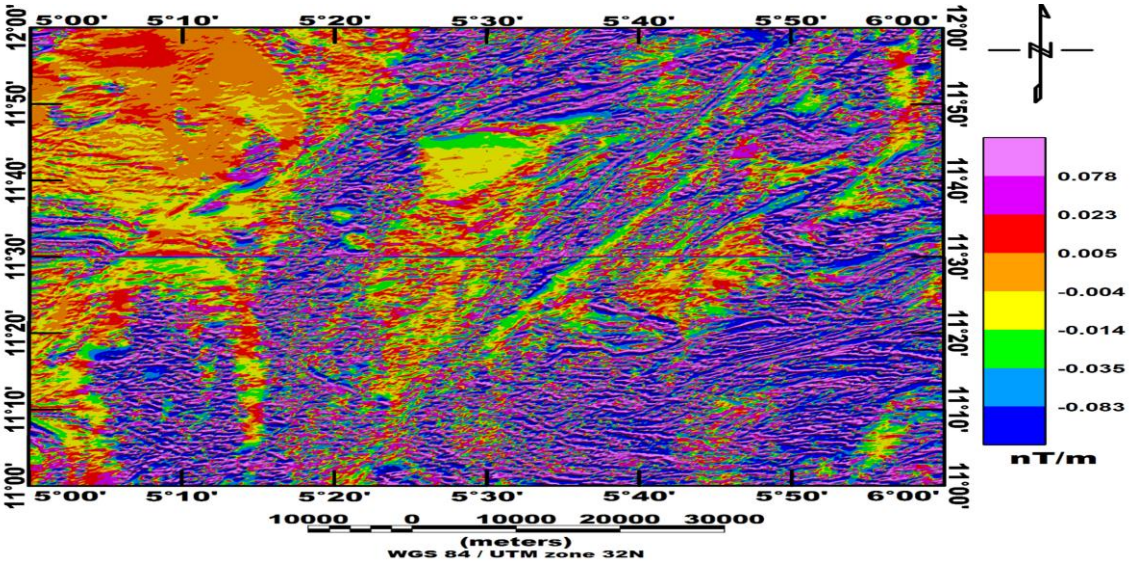

Figure 5a. An illustration of a multi-vector energy systems

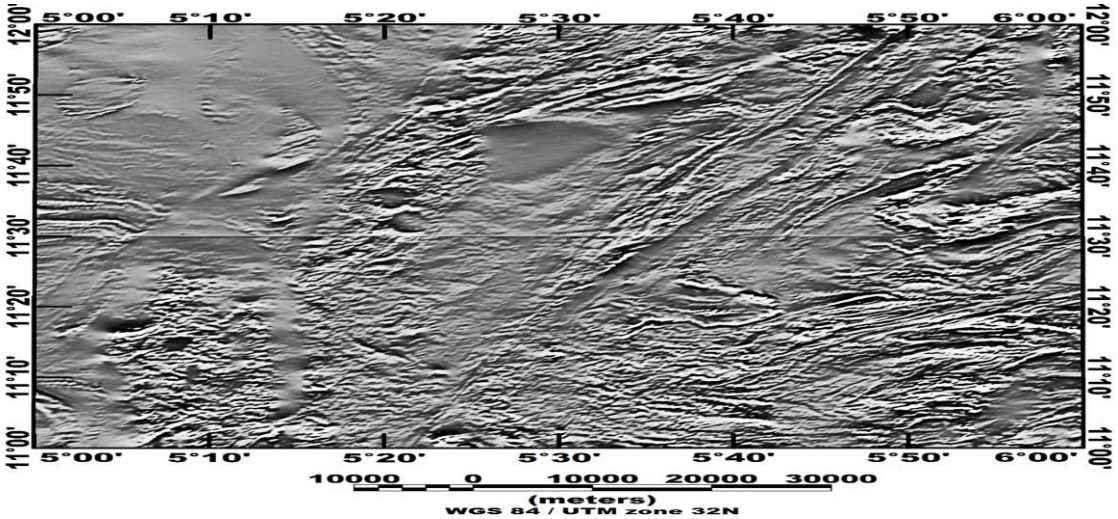

Figure 5b. Grayscale first vertical derivative of the reduced to pole anomaly of the study area

signatures on the reduced to pole map (Figure 4a) are seen as areas of low magnetic signatures on the total field anomaly map (Figure 2) and vice versa. Thus, the similarity that exists between the analytic signal maps (Figure 3a) and reduced to pole map (Figure 4a) has suggested that both techniques has aided in placing the magnetic source anomalies directly above their causative sources.

The reduced to pole anomaly data were further used to produce lineaments map (Figure 4b) of the study region. The produced reduced to pole lineaments (Figure 4b) is similar to those depicted from analytic signal structural trends (Figure 3a) dominantly in the NNE-SSW, NE-SW, E-W and N-S directions. The E-W trends are related to 2000 Ma Eburnean deformation episode (D1) and the NNE-SSW, NE-SW and N-S trends are related to the 600 Ma Pan-African deformation episode (D2). Thus, implying that

the mineralisation zones over the study region are structurally controlled within the two D1 and D2 deformation episodes are highlighted by Umar (2016) and Salawu *et al*. (2019) that worked at Donko, a portion of the study area [5-6].

The first vertical derivative (FVD) of the reduced to pole map (Figure 5a) reveals both negative and positive FVD anomalies of varying amplitudes with values that ranges between -0.083 to 0.078 nT/m. This FVD map (Figure 5a) enhanced the visibility of structural geologic features which were obscured by the long wavelength anomalies in contrast to the total field anomaly map (Figure 2). Evidently, the grayscale colour FVD map (Figure 5b) has aided in showcasing the spatial distribution of the numerous elongated structural geologic features such as; faults and folds. These structural features are more prominent in the north northeast, south southeast and south southwest with NE-SW and E-W trends.

3.2. Quantitative interpretation of the structural geologic features

3.2.1. 3-D Euler deconvolution map

The 3-D Euler deconvolution depths solutions for structural index of one geological model were obtained using window size of 7500 m and

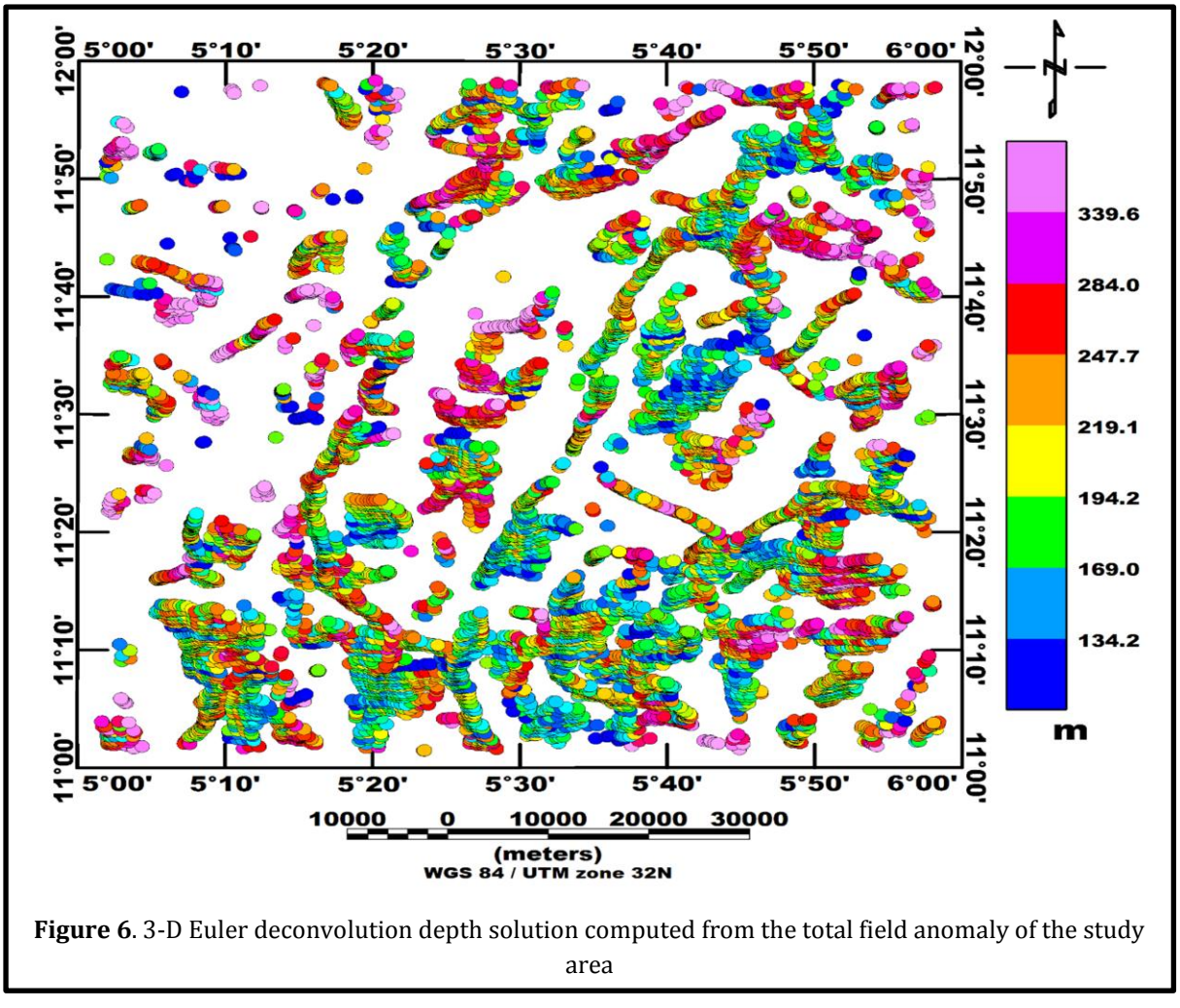

Figure 6. 3-D Euler deconvolution depth solution computed from the total field anomaly of the study area

a depth tolerance of 15 %. The 3-D Euler deconvolution map (Figure 6) shows the possible depths estimates of analytic signal and first vertical derivative structural geologic features with values in the range of 134.2 to 339.6 m. Noticeably, the Euler deconvolution depth solutions are synonymous to the analytic signal (Figure 3a), reduced to pole (Figure 4a) and gray-scale first vertical derivative (Figure 5b) structural features. This suggested that the 3-D Euler deconvolution depth solutions have provided the possible depth extent to the depicted structural features over the studied region. This also reveals similar trends in the NNE-SSW, NE-SW, E-W and N-S directions. These clusters of depth solutions were more prominent in the north northeast, south southeast and south south-western portions of the study area.

4. CONCLUSION

The total field anomaly data of the study area was subjected to the analytic signal and reduce to pole filters in an attempt to correct the magnetic inclination at the latitude region which the study region falls into. Structural lineaments were extracted and compared from both analytic signal and reduced to pole data in order to understand the orientation of the structures controlling the mineralisation of the study area. The rose diagrams of the analytic signal and reduced to pole lineaments reveals that the study area is affected by two deformation episodes which controls the structural trends within the study area. Depth values in the range of 134.2 to 339.6 m were estimated, as the possible depths to the top of the structural features depicted from analytic signal and first vertical derivative anomaly maps. Hence, it was concluded that the potential mineralised zones within the Zuru schist belt, are structurally controlled along the deformed zones. These structurally deformed areas perhaps acts as conduits for the migration and accumulation of numerous potential mineralised deposits.

5. ACKNOWLEDGEMENT

The sincerely appreciate the Nigeria Geological Survey Agency for releasing the data used for the study..

6. CONFLICT OF INTEREST

The authors have declared that there is no conflict of interest.

7. SOURCE/S OF FUNDING

NA

8. REFERENCES

1. Nabighian, M. N. (1972). The analytic signal of two-dimensional magnetic bodies with polygonal cross-section: its properties and use for automated anomaly interpretation. Geophysics, **37**, 507–517
2. Biswas, A (2018). Inversion of source parameters from magnetic anomalies for mineral/ore deposits exploration using global optimization technique and analysis of uncertainty. *Natural Resources research*, **27*(1)***, 77-107
3. Saleh, A., Qudus, B., Magawata, Z.U & Augie, A.I. (2020). Delineation of structural features and depth to the magnetic sources

over Allawa and its environs, Northcentral Nigeria. *International Journal of Advances in Engineering and Management (IJAEM),* **2*(6)***, 545-553

4. Salawu, N. B., Fatoba, J. O., Adebiyi, L. S., Eluwole, A. B., Olasunkanmi, N. K., Orosun, M. M & Dada S. S. (2021). Structural geometry of Ikogosi warm spring, Southwestern Nigeria: evidence from aeromagnetic and remote sensing interpretation. *Geomechanics Geophysics Geo-energy Geo-resources*.**7**:26
5. Salawu, N. B., Olatunji, S., Adebiyi, S. L., Olasunkanmi, K. N. & Dada, S. S. (2019). Edge detection and magnetic basement depth of Danko area, northwestern Nigeria, from low‐latitude aeromagnetic anomaly data. *Springer Nature Switzerland Applied Sciences*, **1**, 1056
6. Umaru, A. O. (2016). Geology and structural evolution of Danko, sheet 74sw part of Zuru schist belt, northwestern Nigeria. Dissertation, Ahmadu Bello University, Nigeria
7. Binta H., Yaro, S. A., Thomas, D. G., Dodo, M. R. (2016). Beneficiation of low-grade manganese ore from Wasagu, Kebbi State, Nigeria. *Journal of Raw Material Resource,* **10*(2)***:63–73
8. Garba, I. (2000). Origin of Pan-African mesothermal gold mineralisation at Birnin Yauri, Nigeria. *Journal of African Earth Sciences*, **31**, 433-449
9. Haruna, I.V. (2017). Review of the Basement Geology and Mineral Belts of Nigeria. *IOSR Journal of Applied Geology and Geophysics (IOSR-JAGG)*. **5*(1):*** 37-45
10. McCurry, P. (1976). The geology of the Precambrian to lower Palaeozoic rocks of Northern Nigeria: a review. In: Kogbe CA (ed) Geology of Nigeria. Elizabethan Publishers, Lagos, pp 15–39
11. Obaje, N. G. (2009). Geology and Mineral Resources of Nigeria, Lecture Notes in the Earth Science Springer: Heidelberg
12. McCurry, P. (1978). Geology of degree sheets 19 (Zuru), 20 (Chafe), and part of 19 (Katsina). Overseas Geological Mineral Resource, Nigeria, p53
13. Turner DC (1983) Upper Proterozoic schist belts in the Nigerian sector of the Pan-African Province of West Africa. *Precambrian Res* **21**:55–79.
14. Akulga, C. (2013). Investigating Gold Mineralization Potentials in Part of the Kibi-Winneba Belt of Ghana using Airborne Magnetic and Radiometric data: unpublished M.Sc. Thesis, Kwame Nkuru University
15. Macleod, I. N., Jones, K & Dai, T.F. (1993). 3-D Analytic signal in the Interpretation of Total Magnetic Field data at low Magnetic Latitudes. *Exploration Geophysics*, **24*(4)***, 679 688
16. Thompson D. T. (1982). EULDPH: a new technique for making computer assisted depth estimates from magnetic data. *Geophysics*, **47*(1):*** 31-37
17. Li, X. (2006). Understanding 3D analytic signal amplitude. *Geophysics*, **71*(2)***, L13–L16
18. Li, X. & Pilkington, M. (2016). Attributes of the magnetic field, analytic signal, and monogenic signal for gravity and magnetic interpretation. *Geophysics,* **81*(6)***, J79–J86.